CGU HS Committee on River Ice Processes and the Environment
19th Workshop on the Hydraulics of Ice Covered Rivers
Whitehorse, Yukon, Canada, July 9-12, 2017.

Measurement of Ice Covers under Moving Loads

Gary Van Der Vinne[1], Michel Lanteigne[2], and James Snyder[3]

[1]*Northwest Hydraulic Consultants Ltd, 9819 12 Ave SW, Edmonton, Alberta T6X 0E3*
gvinne@nhcweb.com

[2]*AECOM Canada Ltd, 4916 47 St, Yellowknife, Northwest Territories, Postal/Zip Code*
michel.lanteigne@aecom.com

[3]*Northwest Hydraulic Consultants Ltd, 9819 12 Ave SW, Edmonton, Alberta T6X 0E3*
jsnyder@nhcweb.com

ABSTRACT

This paper describes the results of field tests carried out to measure the behavior of ice covers under moving vehicle loads for a range of load configurations and bed conditions. The goal of this study was to provide further understanding of the physical processes involved so that transportation on ice covers could be improved. Instrumented test tracks were set up on a number of lake ice covers to record time-series of ice cover deflection, water pressure and extreme fibre ice strain as loaded trucks travelled along the test tracks at various speeds. Tests were carried out for a range of ice thicknesses and water depths as well as for trucks leaving and approaching the shoreline. Tests were carried out with single trucks, B-trains and groups of three closely spaced trucks.

The measurements show how the interaction of ice deflection and water pressure changes as vehicle speed increases and also how the presence of a shoreline, vehicle length and number of vehicles can change the shapes of these responses. Strain measurements show how ice strain relates to ice deflection and water pressure and how the maximum tensile strain shifts from the bottom extreme fibre to the top extreme fibre as vehicle speed increases.

1. Introduction

Floating ice covers are used for winter transportation in cold regions because they provide road connections across rivers and lakes during winter when ferries are not able to operate or when temporary access to a remote site is required for resource extraction. Often, these ice bridges and ice roads are used to haul large numbers of heavy loads such as fuel supplies to remote communities or mine sites. The volume of material that can be hauled over a winter season is limited by the length of time that the ice road can safely remain open. The length of time that these roads are open will be reduced by the increased temperatures associated with climate change. A better understanding of the behavior of these floating ice covers under moving loads could result in more efficient use of the ice covers.

Floating ice covers support vehicle loads with the buoyancy of the ice spread over a larger area due to the stiffness of the ice sheet. A deflection bowl forms under and around the load which displaces the water and hence, provides buoyancy to support the load. Under static loads, the ice deflects until there in a balance between the load and the buoyant force. When loads move, the displacement of water under the deflection bowl also becomes a factor. The interaction between the deflection bowl and the water causes the bowl to change shape as the speed of the load changes. Near the critical speed, the amplitude of the deflection and the curvature of the ice cover are magnified. At speeds higher than the critical speed, deflections are reduced.

There have been many previous field studies about moving loads on ice covers. Wilson (1955) used a deflectometer to measure displacement of ice as vehicles passed by at various speeds. Eyre (1977) also used deflectometers to measure ice deflection over a range of vehicle speeds. Beltaos (1978) used a slope transducer to measure ice deflection. These studies indicated that ice deflections increased at a critical speed and then decreased as speeds increased further. They also indicated that critical speed was a function and water depth and ice thickness.

2. 2012 Testing Program

The 2012 testing program was carried out on the Tibbitt to Contwoyto Winter Road north of Yellowknife in the NWT. Four sets of tests were carried out, two on February 28 and 29, 2012 and two on March 20 and 21, 2012. The water depths and ice thicknesses for the tests are summarized in Table 1. The tests on Waite Lake were carried out in shallow water near shore with the test vehicles going in both directions to obtain data both approaching and leaving the shoreline.

Table 1 Summary of 2012 site characteristics at test center

Test	Date	Location	Ice Thickness (m)	Under Ice Water Depth (m)	Air Temperature (°C)	Vehicle Weight (kg)
1	Feb 28	Ross Lake	1.19	14.4	-10	21,500
2	Feb 29	Waite Lake	1.17	0.9	-16	21,500
3	Mar 20	Ross lake	1.40	4.2	-14	16,700
4	Mar 21	Waite Lake	1.32	0.9	-17	31,120

The equipment set-up and test procedure for each test was similar. A 200 mm hole was drilled through the ice and a 25 mm diameter steel pipe was lowered through the hole and pushed into the lake bed to provide a stable reference point for the tests. A pressure probe with an accuracy of ±0.8 mm was attached to the pipe 0.5 m below the water surface for the first pair of tests and 0.8 m below the water surface for the second pair of tests. A draw wire with an accuracy of ±1.0 mm was attached to a wooden platform fixed to the ice and the wire attached to the pipe above the ice surface. Both the pressure probe and draw wire were attached to a data-logging system capable of logging at a frequency of 10 Hz. The apparatus was housed in a heated Plexiglas box placed over the hole in the ice to provide a less harsh operating environment and to keep the hole from refreezing.

During each test, a number of runs were carried out with vehicle speeds ranging from 5 km/hr to 80 km/hr. Vehicle speed was measured using an RTK GPS antennae mounted on the vehicle. A proximity sensor, set horizontally about 0.6 m above the ice to be triggered by the truck passing by the measuring station, was used to synchronize the GPS clock to the data recorder clock.

The loaded vehicle originally consisted of a tandem axle water truck. On the last day of the second round of tests, the water truck was replaced with a gravel truck in order to have a heavier and more consistent weight (as the water truck continually let water out to keep the pump from freezing).

3. 2015 Testing Program

The 2015 testing program was carried out at three different sites on Prosperous Lake, north of Yellowknife. Three days of tests were carried out from March 7 to 9. The maximum air temperature was between -8°C and -10°C on these three days and the minimum temperature was -18°C on each of these days; however, the previous week the minimum air temperature reached -34°C The three sites were selected to provide a range of water depths below the ice. Tandem axle gravel trucks were used for the all the tests.

Table 2 Summary of 2015 site characteristics at test center

Test	Date	Location	Ice Thickness (m)	Under Ice Water Depth (m)	1st Truck Weight (kg)	2nd Truck Weight (kg)	3rd Truck Weight (kg)
1	April 7	Prosperous Lake	1.51	27.1	24,560	21,970	23,120
2	April 8	Prosperous Lake	1.64	3.25	24,360	21,600	23,200
3	April 9	Prosperous Lake	1.57	6.63	24,700	23,200	20,950

Strain gauges were installed at all the sites at least one day before the tests were carried out so that they would be well bonded to the existing ice. Each of these strain gauges consisted of a full Wheatstone bridge circuit (to compensate for temperature and bending strain) mounted on a 150 mm rod with a 100 mm by 13 mm anchor plate at each end. The bridge circuit consisted of four active 350 ohm strain gauges with a range of ±3000 microstrain (με). Two strain gauges (in-line and perpendicular) were pre-frozen together into 180 mm diameter by 50 mm thick ice pucks for later installation into 200 mm holes drilled into the ice. One puck was installed in a dry hole 75 mm from the bottom of the ice and then frozen into the surrounding ice. An additional 75 mm of water was frozen above the puck but the remainder of the drill hole was left empty to ensure that the ice around the puck was well frozen. A second puck was installed in the top of the ice in a 150 mm deep hole offset about 0.5 m from the bottom puck hole.

On the day of each test, three additional holes were drilled in the ice to install pressure probes and draw wires to measure water pressure and ice deflections. The holes were drilled in a line perpendicular to the ice road, in line with the top strain gauges. The first hole was located about 0.5 m away from the top strain gauge hole, while the second and third holes were about 6 m and 12 m away respectively. The pressure probes and draw wires were referenced to the lake bottom by attaching them to a weighted wire. At each hole, a 9 kg weight was attached to the 1.6 mm diameter wire rope and lowered to the lake bottom. The wire rope was then placed over a pulley which was mounted above the ice and then attached to a 4.5 kg counterweight. A pressure probe with an accuracy of ±0.8 mm was mounted onto a 13 mm diameter wooden dowel which was clamped to the wire rope so that the pressure probe could be positioned below the water surface at a fixed elevation. The pressure probes at Holes 1 and 3 were placed 0.9 m below the water level but the probe at Hole 2 was placed only 0.4 m below the water because the cable on this probe was shorter. A draw-wire displacement sensor with an accuracy of ±1.0 mm was attached to the base of a wooden platform which was in turn screwed to the ice above the hole in the ice. The wire was then attached to the top of the wooden dowel to provide a fixed reference elevation for the draw-wire.

Each hole was covered with a bottomless ice fishing tent with heat supplied by a propane heater. A larger tent was place over Hole 2 which also accommodated the data recording equipment. This equipment consisted of two data-loggers attached to a laptop computer. The strain gauges and pressure probes were connected to one data-logger while the draw-wires were connected to a second data-logger. Both data-loggers recorded at a frequency of 10 Hz. A proximity sensor was mounted horizontally about 0.3 m above the ice so that it was triggered by the truck wheels passing by the measuring station. The signal from the proximity sensor was connected to both data-loggers to provide a common reference between them and to synchronize the data recorder clocks to the GPS clock.

Truck speeds were measured with an RTK GPS antennae mounted on the cab of the lead vehicle. The speeds of the second and third trucks were not monitored. Drivers attempted to maintain a constant spacing between the trucks visually but this was more difficult during the high speed tests.

4. Results and Discussions

The ice deflection, water pressure, and ice strain measurements were recorded as time series as vehicles travelled past the measurement site at various speeds. The time series were transformed to distance from vehicle using the average velocity of the vehicle. In deep water, this transformation provides a snapshot of the ice deflection, water pressure, and ice strain for the speed indicated, with the truck located at the zero distance location which gives an indication of the size and curvature of the deflection bowl. However, near shore where bed elevations were not consistent over the test zone, these graphs should be considered as representing the responses from the ice cover and from the water only at the measuring station as the truck went by. The 2012 data was transformed with the center of the truck at zero distance but the 2015 data was transformed with the front wheel of the lead truck at zero distance.

4.1 Critical Speed

The maximum ice cover deflection varied with vehicle speed, increasing to a maximum value at a critical speed then decreasing again as speed increase further as shown in the example data in Figure 1. The critical speeds obtained from the test data are shown in Figure 2 relative to water depth below the ice. The test data is consistent with results from previous studies. Critical speed increases with depth but is also affected by ice thickness.

The critical speed can be estimated from the equation for the speed of a water wave, V_c, which is a function of the water depth, H and the wave length, L.

$$V_c = \left(\frac{gL}{2\pi}\tanh(\frac{2\pi H}{L})\right)^{1/2} \qquad [1]$$

In shallow water where H/L is small, Equation [1] reduces to a function of depth.

$$V_c = (gH)^{1/2} \qquad [2]$$

In deep water where H/L is large, Equation [1] reduces to a function of wave length.

$$V_c = \left(\frac{gL}{2\pi}\right)^{1/2} \qquad [3]$$

Nevel (1970) assumed the wave length was defined by the width of the deflection bowl which he defined as 5 times the characteristic length of the ice, l_c,

$$l_c = \left(\frac{Eh^3}{12\gamma_w(1-\nu^2)}\right)^{1/4} \qquad [4]$$

where h is the ice thickness, E is the elastic modulus of ice, γ_w is the unit weight of water, and ν is Poisson's ratio.

Figure 3 shows a selection of deflection bowls measured on Ross Lake, on Feb 28, 2012, plotted with dimensionless distance scaled with $2\pi l_c$. At slower speeds, the widths of the deflection were about $2\pi l_c$; but, at higher speeds, the shape of the deflection bowl changed and the width of the deflected zone approached $4\pi l_c$. The best fit with the critical speed data shown in Figure 2 was found to be when the wave length in Equation 1 was set to $4\pi l_c$, assuming E = 9 GPa and ν =0.30. This value of E is the upper limit for the instantaneous response of competent ice – lower, effective values would require an even wider deflection bowls to fit the critical speed measurements in shown in Figure 2.

4.2 Water Pressure vs Ice Deflection

The initial tests carried out on Ross Lake in 2012 on 1.2 m of ice over 14.4 m of water indicated that, at slow vehicle speeds, the shape of the deflection bowl is similar to that of a stationary load and the water pressure remains relatively constant (Figure 1). The maximum deflection is about 10 mm. Above 17 km/hr, the water pressure begins to decrease under the deflection bowl and the ice cover deflections begin to increase. At 44 km/hr, the leading edge to the deflection bowl begins to rise with a corresponding increase in the water pressure at that location. The water pressure and ice deflection have similar shapes and the deflection at the center of the deflection bowl is at a maximum. As well, the water pressure on the trailing edge of the deflection bowl begins to oscillate. At higher speeds, a spike in water pressure forms just ahead of the deflection bowl along with a smaller rise in deflection and the maximum deflection begins to decrease. The behaviour of the ice cover is similar to that of a boat transitioning from displacement mode to on-plane mode. The ice cover can be considered a large, flexible hull traveling through the water.

The variations in water pressure indicate why the changes in deflection occur. At slow vehicle speeds, the water is able to move out of the way as the deflection bowl advances. At high speeds, due to inertia, the water cannot move fast enough to get out of the way of the deflection bowl so the water pressure contributes to the support of the vehicle, reducing the contribution from the buoyancy of the ice. At critical speed, the speed at which the ice deflection is at a maximum, the water pressure is low under the vehicle, so the ice must deflect further to increase its buoyancy to support the vehicle. The water pressure is low at critical speed because the natural frequency of the vertical motion of the water, as described by wave theory, is the same as the frequency of the vertical motion of the ice.

Figure 4 shows the variations of maximum ice deflection and water pressure relative to calculated critical speed as shown in Figure 2. The ice deflections reach a maximum value of 1.8 times the static defection near the critical speed before decreasing to values below the static deflection. Water pressure decreases to values of up to1.5 times the static deflection near the critical speed before switching to positive maximum pressures with maximum values up to 4.7 times the static deflection at valves of 1.5 times the critical speed or more.

4.3 Ice Deflection and Water Pressure Variation Near Shore

Tests were carried out on Waite Lake in 2012 in shallow water about 60 m from the edge of the grounded ice. The first set of tests were carried out on 1.2 m of ice over 0.9 m of water. A second set of tests was carried out on 1.3 m of ice over 0.9 m of water near the same location. The test vehicles were run in both directions to obtain data both approaching and leaving the shoreline.

Figure 5 shows the variations of maximum ice deflection relative to critical speed for both approaching and leaving the shoreline as well as for deep water. The data shows that, while maximum deflections near critical speed were slightly higher in the shallow water, they were in the same range as previous data and there was little difference due to the direction of travel.

Figure 6 shows the variations of maximum change in water pressure relative to critical speed for both approaching and leaving the shoreline, as well as for deep water. The data is presented as absolute values because the maximum and minimum water pressures were similar in many cases.

The data shows that maximum change in water pressures above critical speed were higher in the deep water and there was little difference in water pressure due to the direction of travel for the shallow water data.

The data collected in shallow water near shore indicates there was little difference in ice deflections and water pressures due to the direction of travel. It was expected that as the shoreline interfered with the ability for the water to be displaced by the deflection bowl that higher deflections or water pressures would be observed. The location of the test sites was about three characteristic lengths away from the shoreline which would place the edge of a slow moving deflection bowl just at the shoreline, so it is possible that the tests were carried out too far from the shoreline to show shoreline effects. Testing nearer the shoreline was not possible because the change in terrain made it unsafe to maintain vehicle speeds approaching the shoreline and difficult to achieve the speeds leaving shore. The lake bed in the vicinity of the shoreline in the tests had a mild slope which may have influenced the results as well.

4.4 Ice Strain

In 2015, tests were carried out at three sites on Prosperous Lake which included ice strain measurements. Four strain gauges were installed at each site to measure strain in-line and perpendicular to the direction of vehicle travel near both the top and bottom of the ice; but, unfortunately, some of the gauges malfunctioned before measurements could be obtained from them. At Sites 1 and 3, the top in-line strain gauge malfunctioned so this important measurement was only available at Site 2 with the shallowest water. The top perpendicular strain gauge at Site 2 malfunctioned as did the bottom perpendicular strain gauge at Site 1.

Selected strain gauge data from Site 2 above 3.25 m of water are shown in Figure 7 along with ice deflection and water pressure data for reference. At speeds well below the critical speed of 20 km/hr, the maximum top in-line (TI) strain of -43 $\mu\varepsilon$ (negative strains indicate compression) was somewhat higher than the maximum bottom in-line (BI) strain of 34 $\mu\varepsilon$; however, the tensile strain is likely the more critical value because the tensile strength of ice is less than the compressive strength. The maximum TI tensile strain, of 12 $\mu\varepsilon$ occurred at the inflection points nearer to the front and rear of the deflection bowl. At a speed near the critical speed, the TI tensile strain at the front of the deflection bowl of 36 $\mu\varepsilon$ was higher than the BI tensile strain under the vehicle of 30 $\mu\varepsilon$ but not as great as the TI compressive strain of 43 $\mu\varepsilon$ under the vehicle. At speeds higher than critical speed, both the TI and BI strains decreased in magnitude.

Selected strain gauge data from Site 3 above 6.63 m of water (V_c=29 km/hr) are shown in Figure 8. This data indicates that the bottom perpendicular (BP) strains were typically much lower than the BI strains and did not change significantly with vehicle speed. The top perpendicular (TP) strains were also more consistent in shape and, while the maximum value varied with vehicle speed, it was always in compression.

Figure 9 shows variation of the maximum in-line tensile strains with fraction of critical speed. The greatest BI tensile strains occurred when the vehicle was near critical speed or lower and tended to decrease at higher speeds. The maximum TI tensile strains were highest at about 2.5 times the critical speed and were of similar magnitude to the maximum BI tensile strains near critical speeds. As vehicle speed increases towards critical, tensile strain is greatest at the bottom of the ice cover under the vehicle; but, as vehicle speed increases beyond 1.8 times critical, tensile strain becomes greatest at the top of the ice cover, at the rise in the ice sheet located ahead of the truck.

One difference between BI and TI tensile strains is that the TI strains as subject to additional tensile strains due to contraction of the ice cover with rapidly cooling air temperatures. The BI tensile strains may also increase when the temperature increases again but only if open cracks on the surface have been filled with water and refrozen.

5. Summary and Conclusions

Critical speed on an ice cover can be estimated from the equation for the speed of a water wave, where the wave length is a function of the width of the deflection bowl. The best fit with the data was found to be when the wave length was set to 4π times the characteristic length of the ice, or two times the width of the deflection bowl at slow speeds.

The water pressure measurements indicate why the changes in maximum deflection occur with changes in vehicle speed. At slow vehicle speeds, the vehicle is supported by the buoyancy of ice while at high speeds water pressure supports much of the load. At critical speed, the water pressure is low and the ice deflection at a maximum because the natural frequency of the vertical motion of the water as described by wave theory is the same as the frequency of the vertical motion of the ice.

The data collected in shallow water near shore indicates there was little difference in ice deflections and water pressures due to the direction of travel. Testing nearer the shoreline was not possible because the change in terrain made it unsafe to maintain vehicle speeds approaching the shoreline and difficult to achieve the speeds leaving shore.

The critical speed decreases significantly near shore as the water becomes shallower. Vehicles must pass through the critical speed as they go onto and off the ice. Therefore, as a truck crosses a body of water both ice deflections and water pressures increase at some point near the shoreline and these increases may cause increased tensile strains in the ice.

The strain data indicate that tensile strain does not increase as much as ice deflection at critical speed. Therefore, limiting vehicle speeds to values well below critical may not increase safety significantly enough to justify the longer travel times. It may be more economical to increase design ice thicknesses slightly or reduce loads to accommodate a 20% increases in strain rather than limiting speeds. Also, given that it was also observed that vehicles pass through critical speed each time they enter and exit the ice surface, limiting speeds below critical over the rest of the ice sheet does not appear to decrease the risk of ice failure significantly.

Strain data obtained at the top of the ice cover are limited in this study, given that only one out of three in-line (TI) strain gauges and two out of three perpendicular (TP) strain gauges were operational. Additional testing is required to obtain a better understanding of tensile strain at the top of the ice sheet and the consequences of exceeding critical speeds. Measurements, including strain measurements nearer the shoreline and with a wider range of shoreline conditions, are also required to confirm that the presence of shorelines do not significantly change the behavior of the ice under moving loads. The effects of temperature changes on the tensile strains in the ice should also be investigated.

References

Beltaos, S., 1978. *Field studies on the response of floating ice sheets to moving loads*. Transportation and Surface Water Engineering Division, Alberta Research Council Contribution Series 938, Edmonton, AB.

Eyre, D., 1977. *The flexural motion of a floating ice sheet induce by moving vehicles*. Journal of Glaciology 14.

Nevel, D.E., 1970. *Moving loads on a floating ice sheet*. US Army Corp of Engineers, Cold Regions Research and Engineering Laboratory, Research Report 261, Hanover, N.H.

Wilson, J.T., 1955. *Coupling between moving loads and flexural waves in floating ice sheets*. US Army Corp of Engineers, Cold Regions Research and Engineering Laboratory, Snow Ice and Permafrost Establishment Report 34, Hanover, N.H.

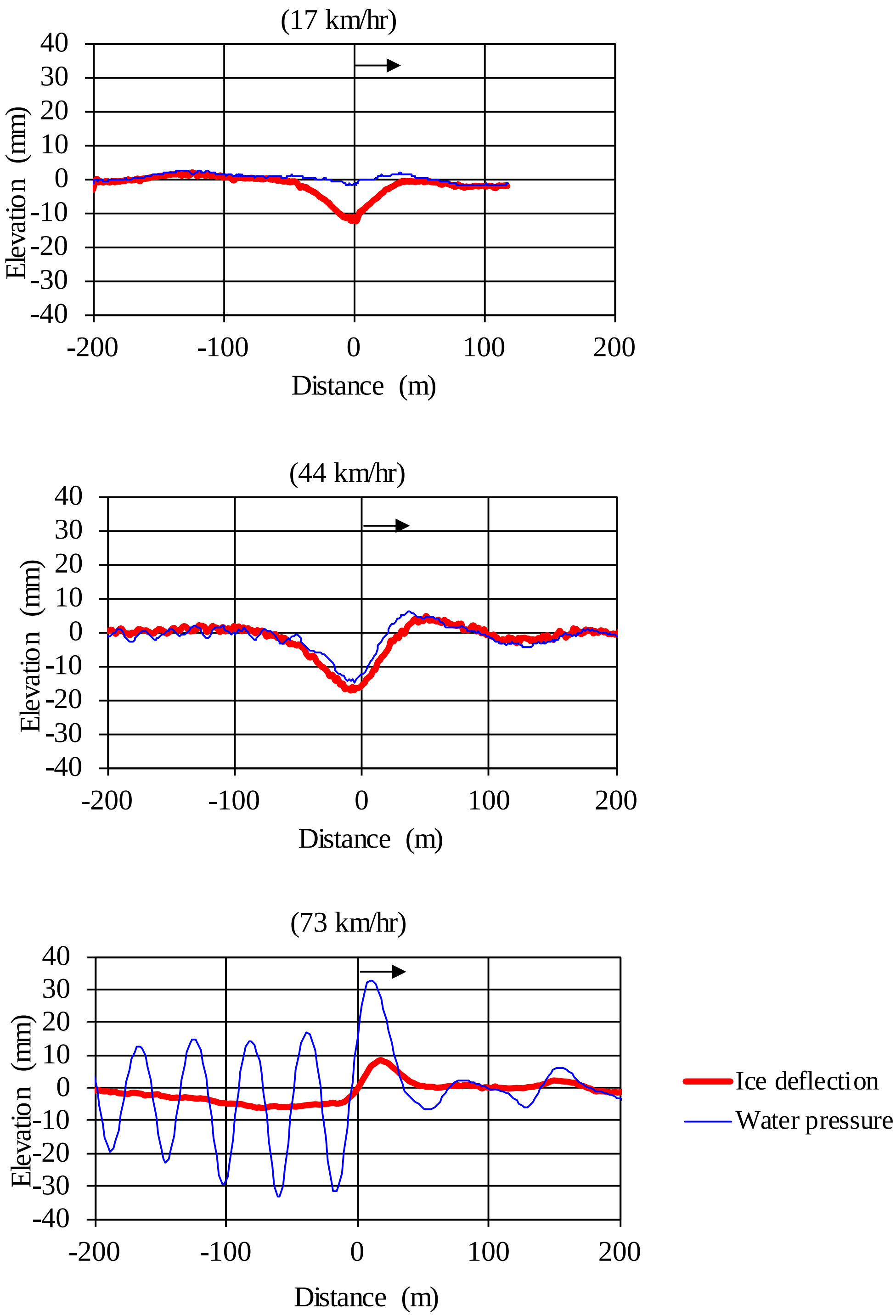

Figure 1. Variation of ice deflection and water pressure with distance from vehicle on Ross Lake on Feb 28, 2012 with a critical speed of 43 km/hr

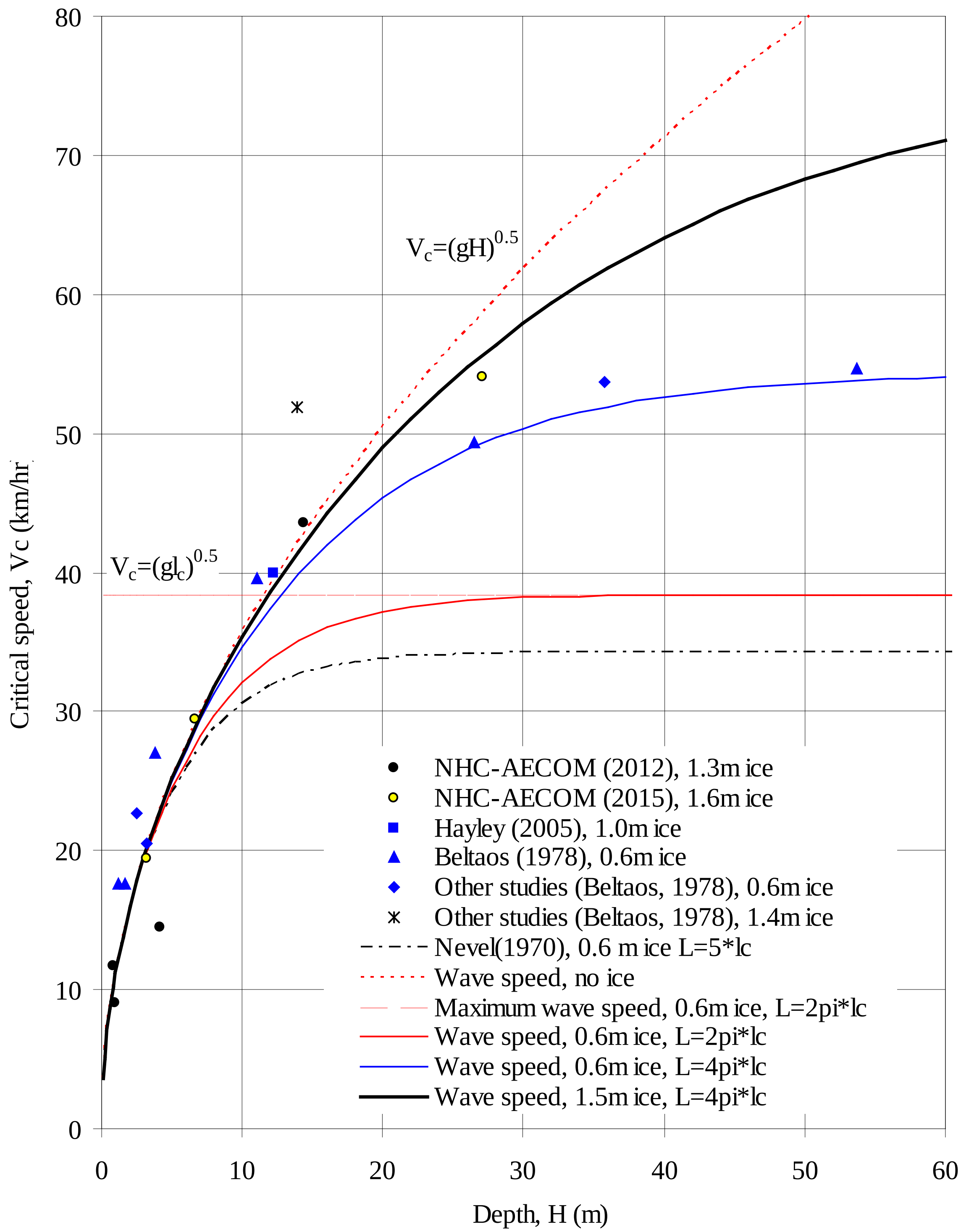

Figure 2. Variation of critical speed with water depth, H and wavelength, L.

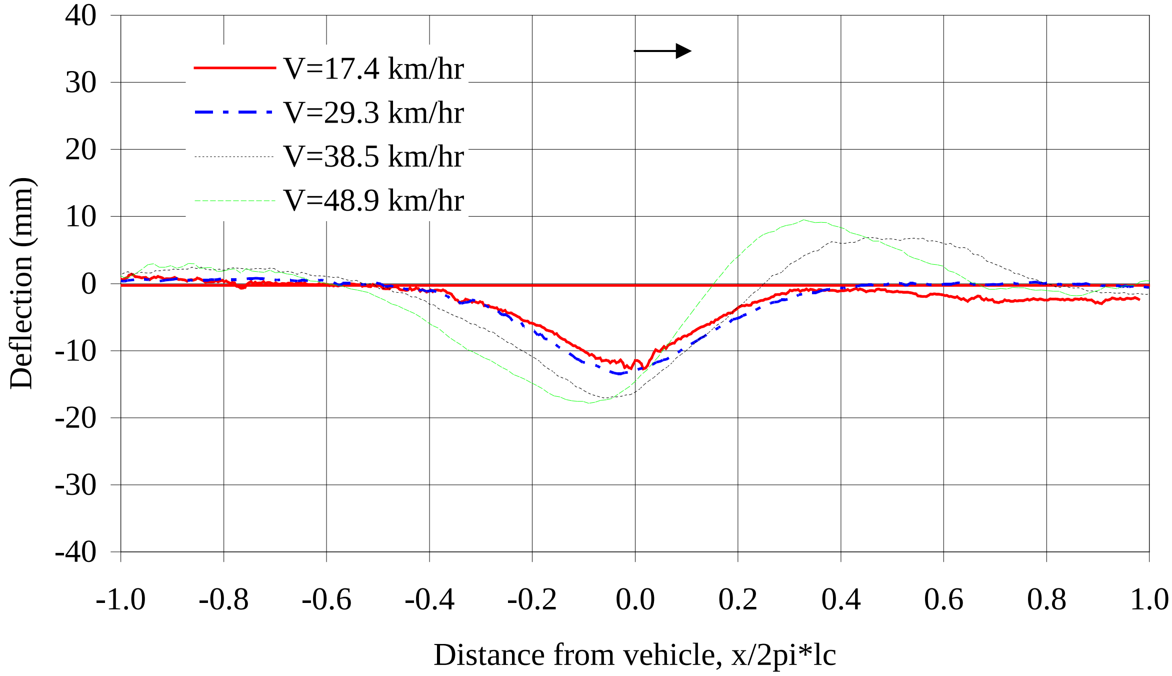

Figure 3. Variation in shape of deflection bowl with vehicle speed.

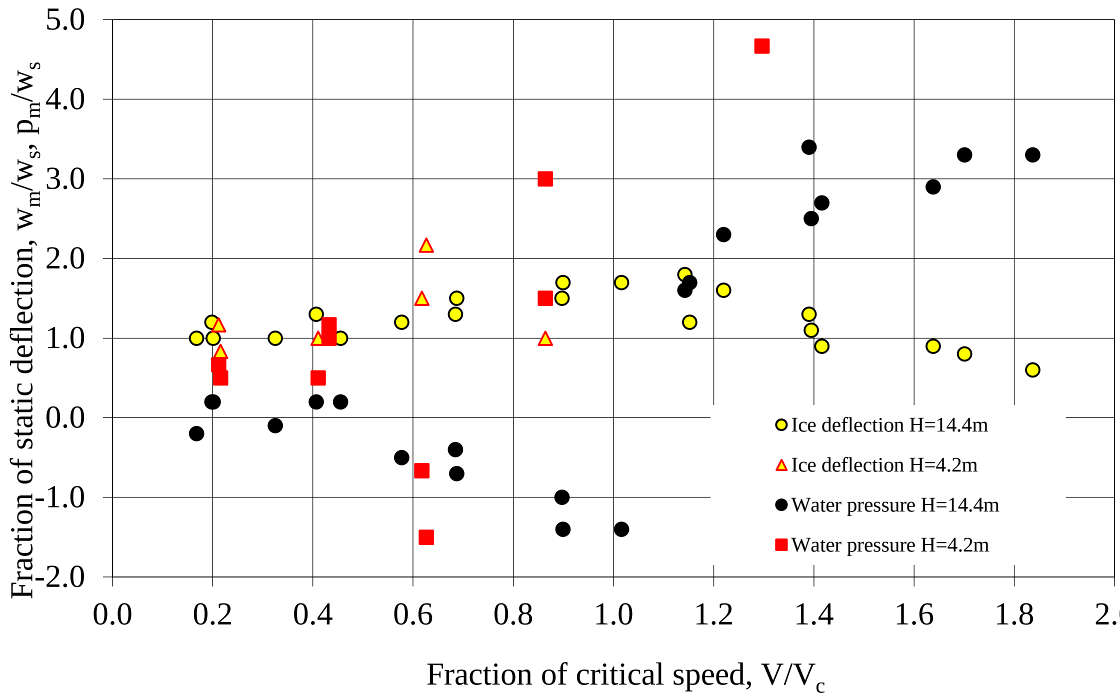

Figure 4. Variation of maximum ice defection and water pressure with vehicle speed on Ross Lake for water depths, H of 4.2 m and 14.4 m.

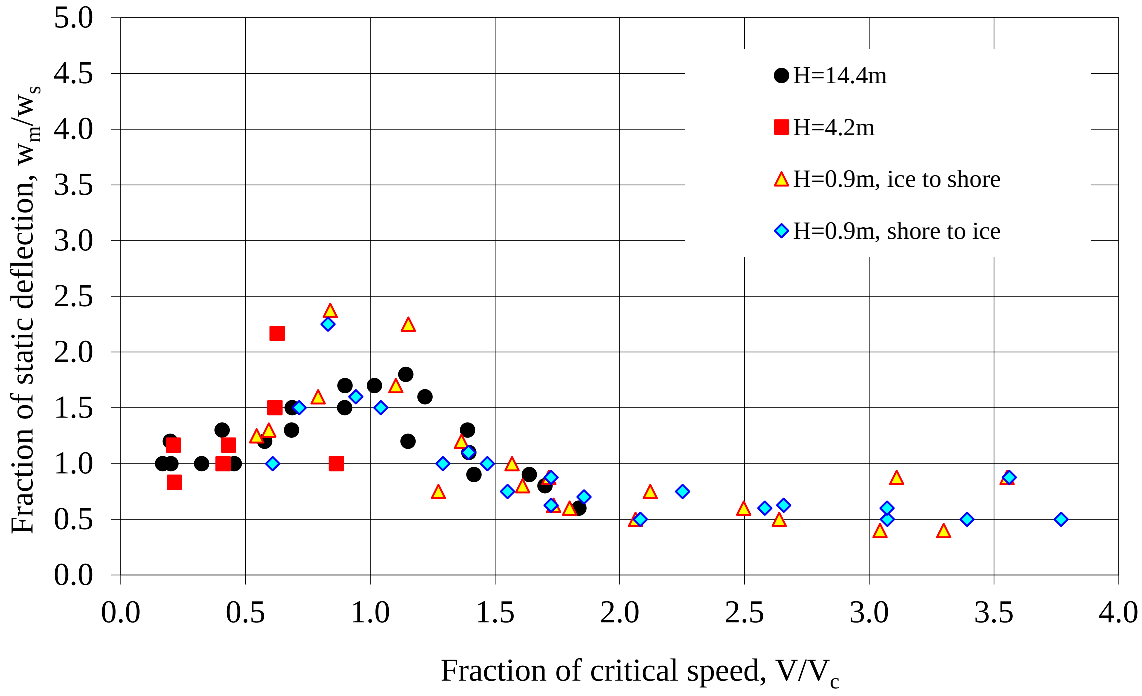

Figure 5. Variation of maximum ice deflection with vehicle speed for various water depths, H.

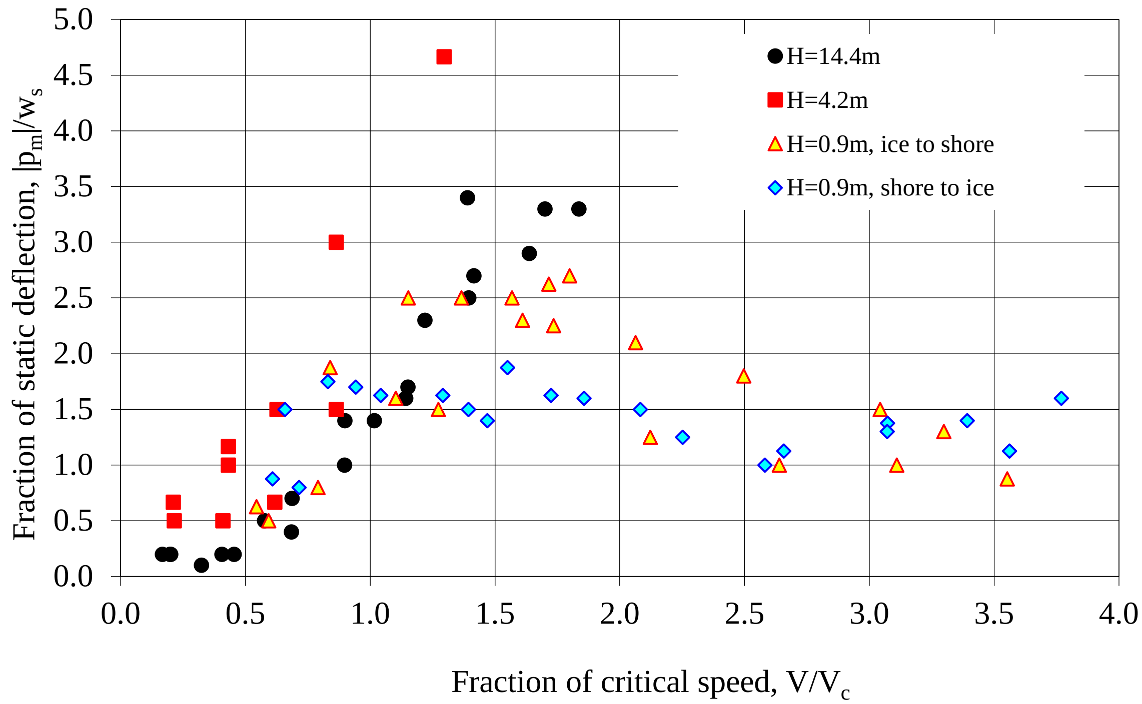

Figure 6. Variation of maximum water pressure with vehicle speed for various water depths, H.

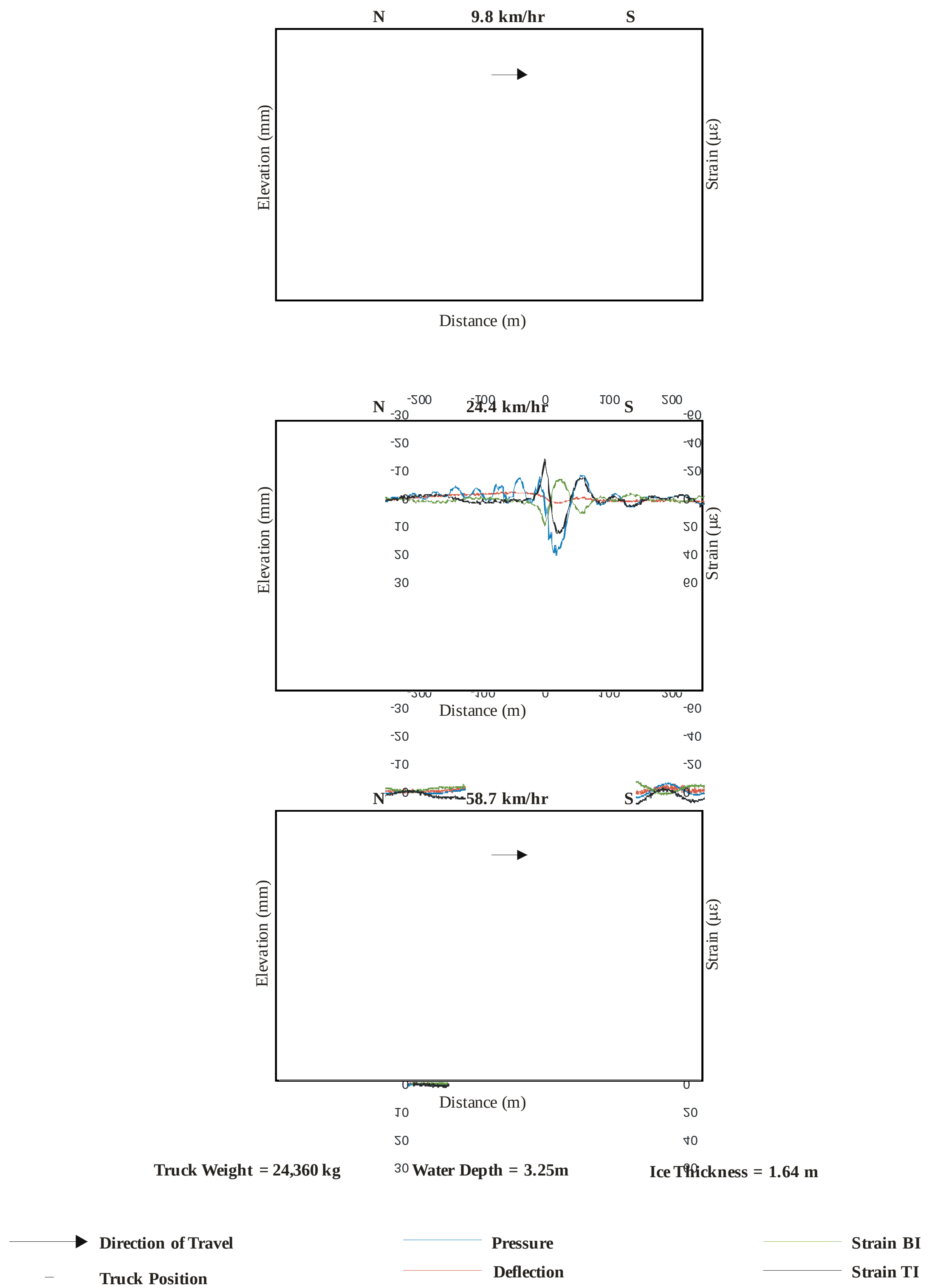

Figure 7. Variation of in-line strains, water pressure and ice deflection with distance from vehicle at Site 2 on Prosperous Lake (V_c = 20 km/hr).

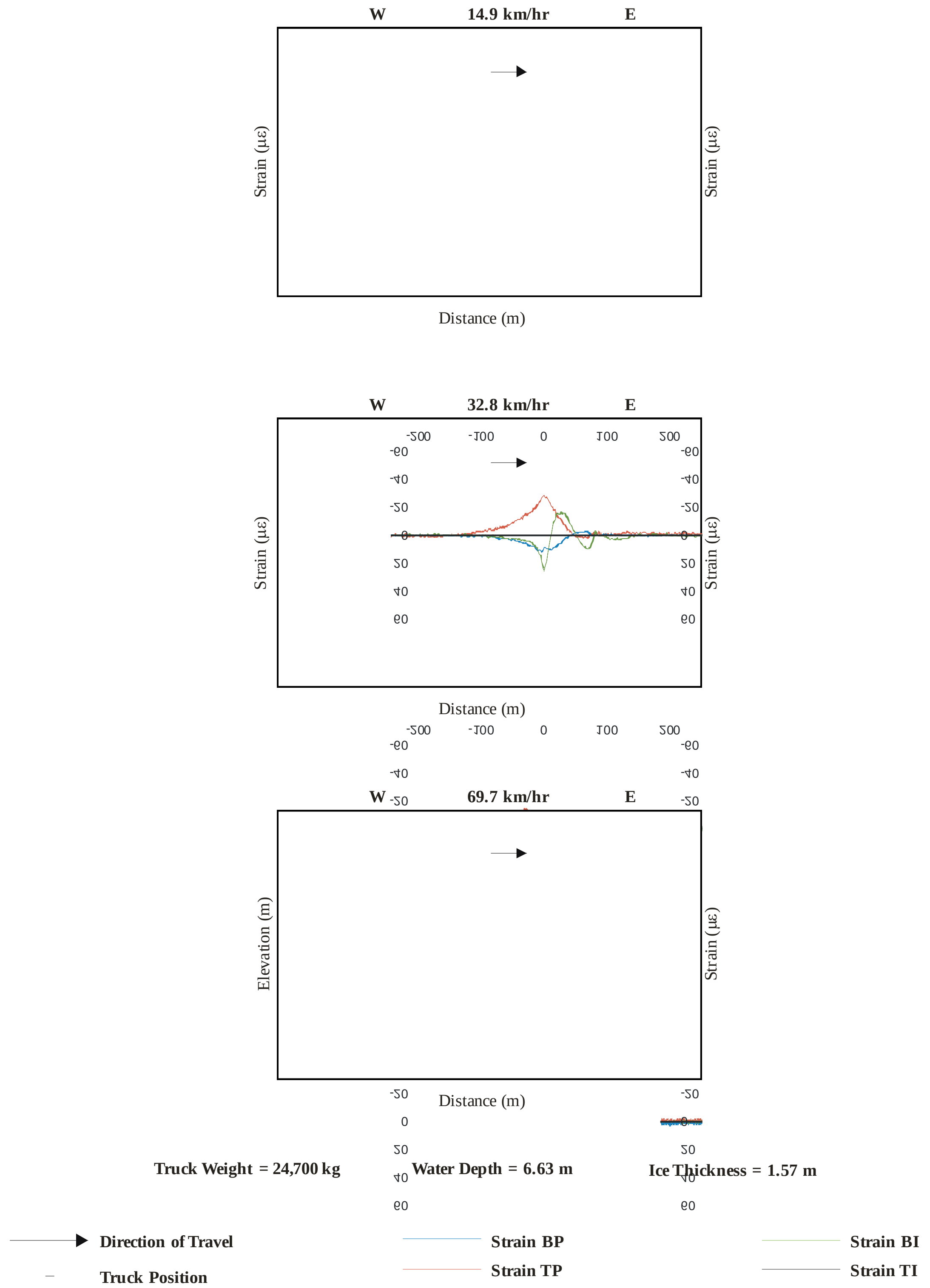

Figure 8. Variation of strains with distance from vehicle at Site 3 on Prosperous Lake (V_c = 29 km/hr).

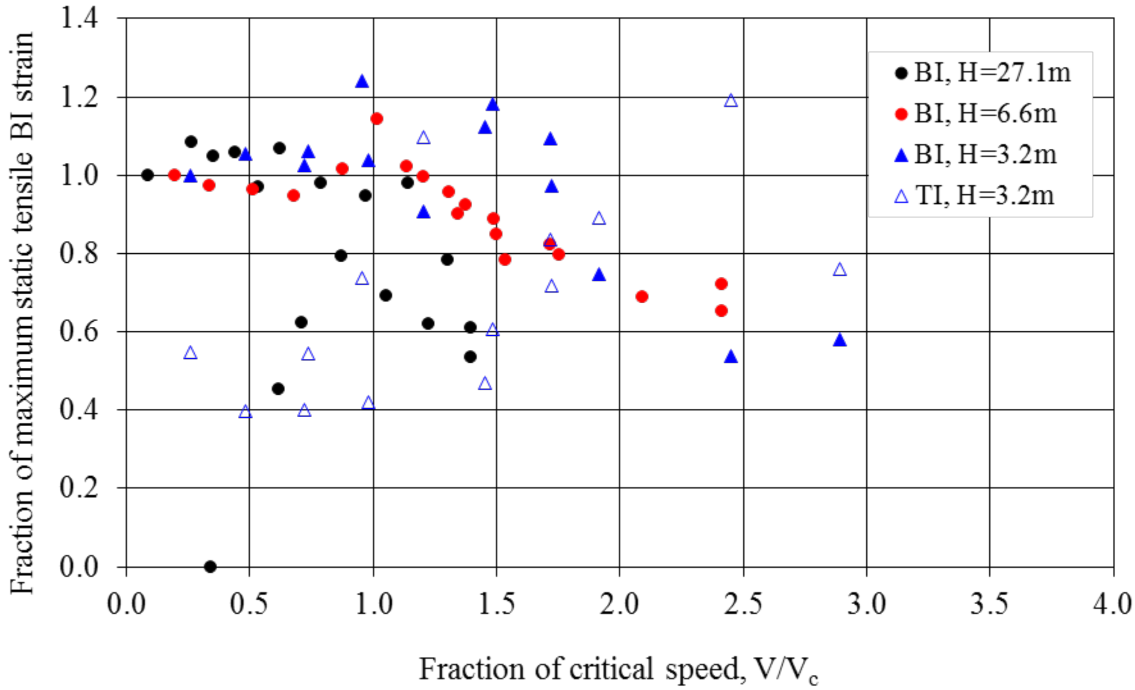

Figure 9 Variation of maximum in-line tensile strain with vehicle speed.